Environmental Science and Pollution Research (2023) 30:120793–120804
https://doi.org/10.1007/s11356-023-30643-0

RESEARCH ARTICLE

Desorption kinetic and sequential extraction of Pb and Zn in a contaminated soil amended with phosphate, lime, biochar, and biosolids

Matheus Sampaio Carneiro Barreto[1,2] · Frederico Prestes Gomes[2] · Hudson Wallace Pereira de Carvalho[3,4] · Luís Reynaldo Ferracciú Alleoni[2]

Received: 3 July 2023 / Accepted: 19 October 2023 / Published online: 9 November 2023

Abstract

The mining and metallurgical industry sector activities often release potential toxic elements (PTE) surrounding exploitation area. We evaluated the addition of phosphate and lime using the dosage of 0.5:1, 1:1, and 2:1 molar ratio of PO_4^{3-} and CO_3^{2-} to the sum of PTE, respectively, and also, biochar and biosolids using the dosage of 2.5, 5, and 10% (m:m) to immobilize PTE in contaminated forest soil (Pb (270 mg kg^{-1}) and Zn (858 mg kg^{-1})) near an abandoned mine site in Brazil. The desorption by stirred flow kinetics revealed that 15% of the total Zn and 12% Pb contents are mobile before any amendment application. Phosphate amendment decreased Pb desorption but increased Zn desorption. Biochar and biosolids immobilize high amounts of Zn and Pb because of their high cation exchange capacities and alkaline properties; however, 20% biosolid dose increased Pb desorption. X-ray absorption spectroscopy suggested Zn-kerolite as the major species in the contaminated soil, likely from mine dust. The change in Zn speciation after soil amendment addition indicated that biochar and lime kept a high proportion of Zn-Al species, whereas phosphate and biosolids led to more Zn-Fe species. Our results pointed out that lime might reduce both Pb and Zn mobilities; however, field trials are crucial to confirm the immobilization efficiency of lime and other amendments over long term.

Keywords Soil pollution · Mining soil reclamation · Remediation · Spectroscopy · Sequential extraction

Introduction

Mining and metal processing activities provide the raw materials necessary for metallurgical industries to manufacture products such as electronics, energy storage, and transportation, which are essential devices for modern lifestyles. These activities offer numerous benefits to society, including economic development (Ali et al. 2017). For instance, the Brazilian mining sector contributes nearly 12% to the country's gross domestic product (Brazilian Economy Ministry 2022; Gardioli et al. 2023). However, soil pollution caused by potentially toxic elements (PTE) is an undesirable side effect of mineral exploration activities (i.e., mining and ore refinement) and had been an environmental concern in many parts of the world (Ettler 2016; Kalisz et al. 2022; Kennedy et al. 2023), not only in loco (i.e., mine spot) but also spreading to the surrounding areas through windblown dust deposition (Ono et al. 2016; Naz et al. 2018; Entwistle et al. 2019). Once these PTE are remobilized from soil and sediments, they might migrate to groundwater, plants, animals, and finally humans, posing a potential threat to public health (Chen et al. 2022; Li et al. 2023).

Soil contamination is a major environmental concern that requires action in prevention and urgent remediation to avoid PTE spreading and possible damages to ecosystems. There is a strong interest in developing strategies and methods to

Responsible Editor: Kitae Baek

✉ Matheus Sampaio Carneiro Barreto
mbarreto@udel.edu

[1] Department of Plant & Soil Sciences, University of Delaware, 476 Harker ISE Lab, Newark, DE 19716, USA

[2] Luiz de Queiroz College of Agriculture, University of São Paulo, Av. Pádua Dias, 11, São Paulo, Piracicaba 13418-900, Brazil

[3] College for Sustainable Agriculture and Environmental Science, Mohammed VI Polytechnic University, BenGuerir 43150, Morocco

[4] Centre for Nuclear Energy in Agriculture, University of São Paulo, Avenida Centenário, São Paulo, Piracicaba 303, 13416-000, Brazil

ameliorate contaminated soils and prevent PTE spreading, such as landfilling and excavation; however, these actions are often expensive and environmentally unfeasible (Vareda et al. 2019; Rajendran et al. 2022). The amendments reduce the PTE mobility due to adsorption, complexation, and precipitation mechanisms, making them less available for human and plant uptake and less prone to leaching into groundwater (Bolan et al. 2003; Kumpiene et al. 2008). Utilizing soil amendments for in situ PTE immobilization is profitable and environmentally friendly option because (i) it is low invasive, as it is focused on soil surface (i.e., ~ 20 cm, after soil tillage), (ii) it is applicable for a wide number of inorganic pollutants (Zhai et al. 2018; Vrînceanu et al. 2019; Gao et al. 2023), and (iii) it is affordable ($40–$65/m^3 of soil (Martin and Ruby 2004), €45–€170/m^3 (Liao et al. 2022)), if compared to other remediation options such as electrokinetic ($26–$295/m^3 (Federal Remediation Technologies RoundTable 2009), ~ $200/$m^3$ (Reddy and Cameselle 2009)), vitrification ($300–$500/m^3 (USEPA 2004), 120–680/m^3 (Reddy and Cameselle 2009)), phytoremediation ($25-$100/m^3 (USEPA 2004), $626–$2322/m^3 (Robinson et al. 2015), ~ $250/$m^3$ (Reddy and Cameselle 2009), or solidification ($87–$190/m^3, (Wan et al. 2016)). It is noteworthy that updated values of remediation cost are ignored or not presented in recent literature.

Several amendment studies have been dedicated to evaluating the PTE's ability to immobilize in soil and decrease its environmental risks, such as the application of phosphate (He et al. 2013), alkaline materials (Lee et al. 2009), biochar (Puga et al. 2016), and biosolids (Basta et al. 1997). However, soil contamination with multiple PTE is a crucial challenge for soil remediation technologies because of the interactions among the soil properties, the chemical behaviors of each PTE (e.g., solubility and redox variations), and the soil amendment reactions. All these factors may lead to conflict when attempting immobilization multiple contaminates (Fang et al. 2016; Wang et al. 2019). In our previous study, we evaluated the effectiveness of some soil amendments for immobilizing lead (Pb) in mine-waste impacted soil and concluded that phosphate and lime decreased Pb desorption and increased the amount of Pb in the fraction with the lowest mobility. However, biochar and biosolids had the opposite effect, resulting in an increase in Pb desorption (Gomes et al. 2022).

For this study, we evaluated the addition of phosphate, lime, biochar, and biosolids to decrease the mobility of the Pb and Zn in an impacted soil under the secondary forest located in the vicinity of an abandoned, heavily polluted mine site in Brazil previously assessed (Gomes et al. 2022). The efficacy of metal immobilization was evaluated by PTE desorption using stirred flow kinetic and sequential extraction approaches. Additionally, the alterations in Zn speciation resulting from soil amendment reactions were investigated using X-ray absorption near edge structure (XANES) spectroscopy. Hence, we expanded the significance and interpretation of remediation strategies presented in our previous study for a heavily contaminated site (PTE in gram per kilogram), for a contamination for both Zn and Pb observed in a forest soil in measured in milligram per kilogram. We expect that the outcomes of our research contribute to the understanding of remediation practices in variated levels of soil contamination by multiple PTE.

Materials and methods

Contaminated forest soil

The soil sample was collected surrounding (less than 1 km distance) a discontinued Zn exploitation area sited in Vazante city, State of Minas Gerais, Brazil (approximately to geographic coordinates 17° 55′ 3″ S, 46° 49′ 2″ W, see Fig. 1SM). This area is covered by a secondary forest of the Brazilian "Cerrado" biome, known as the savanna-like formations, which is composed of xeromorphic, sclerophyllous, and exotic species such as *Eucalyptus*.

Twenty subsamples (~ 500 g) of soil were collected from the superficial soil layer (0–20 cm) at six points along a transect throughout the forest site (Fig. 1SM). The composite sample, hereafter referred to as the forest soil, was air-dried at room temperature (~ 22 °C) and passed through a 2-mm sieve. A portion of the forest soil sample was dispersed by a sodium hexametaphosphate solution (5 g L^{-1}) in mechanical agitation (16 h), and then, the particle size distribution was measured according to Stokes law (Pansu and Gautheyrou 2007). We determined 14% sand, 9% silt, and 77% clay in the soil sample. The major mineral phases identified by X-ray diffractometry (XRD) analysis in the silt and clay fractions were kaolinite, gibbsite, muscovite, goethite, and hematite, while quartz is the main mineral phase in the sand fraction (data not shown).

Amendments and incubation time

Individual portions of the original forest soil (100.0 g) were amended with each soil amendment at different rates. Monobasic ammonium phosphate ($NH_4H_2PO_4$, analytical grade), as a phosphate amendment, was applied evenly to the soil in a 0.5:1 (quarter dose), 1:1 (half dose), and 2:1 (full dose) molar ratio of PO_4^{3-} to the sum of PTE (i.e., Pb, Cd, and Zn both in molar base) as suggested elsewhere for soil amelioration (Cao et al. 2009). Likewise, lime ($CaCO_3$, analytical grade) was added as an alkaline material, at a 0.25:1 (quarter dose), 0.5:1 (half dose), and 1:1 (full dose) molar ratio of CO_3^{2-} to the sum of PTE, as suggested by Basta and McGowen (2004). The biochar was made from

sugarcane (*Saccharum officinarum*) straw pyrolyzed at 450 °C, as detailed by Feola Conz et al. (2017). The rates used were 2.5, 5, and 10% weight-based (m:m; wt%) of biochar, as evaluated previously (Puga et al. 2015, 2016; Ali et al. 2020). Additionally, we tested the residual biosolids produced by a station of water treatment in Piracicaba city (State of São Paulo, Brazil). It was composted, stabilized, and analyzed following the official Brazilian guidelines (MAPA 2014). The rates used for biosolids were 5, 10, and 20% weight-based (mass/mass), as tested by Madejón et al. (2010) and Elkhatib and Moharem (2015). Each combination of amendment type (phosphate, lime, biochar, and biosolids) × amendment rate was carried out in triplicate.

The samples with amendments were well homogenized, and water was added to reach 70% of the maximum water retention capacity (MWRC), along with the forest soil without any amendments (control). All samples were kept incubated at 25 ± 2 °C for 60 days, with the water refilled every 3 days based on mass loss (i.e., water loss ~ 30% MWRC) to conserve the moisture level suitable for chemical reactions.

Soil chemical analysis, desorption, and sequential extraction

Soil chemical analyses were conducted following the incubation period. For all the analyses mentioned below, we replicated the same procedures and protocols used previously (Gomes et al. 2022). Pb and Zn desorption kinetic was measured by the stirred flow method. In brief, 200 mg of the samples (initial forest soil and it amended) was placed in the reactor, a 12-mL stirred flow chamber (Fig. 2SM), and a 25-mm diameter cellulose filter membrane with a 0.45 µm pore size was used in the reaction chamber. The solid and desorption solutions (Mehlich-III: 0.2 M CH_3COOH + 0.25 M NH_4NO_3 + 0.013 M HNO_3 + 0.015 M NH_4F + 0.001 M EDTA) were stirred in the reactor using a magnetic stirrer at 300 rpm, and the liquid portion of it was then flowed through the chamber, passing the filter at a rate of 1 mL min^{-1} with a piston displacement pump designed for use in a high-performance liquid chromatography system, been that the liquid portion was collected at 2-min intervals. The concentration of Pb and Zn was measured by an ICP-OES (Pb emission line at 220.353 nm, calibration curve from 0 to 20 mg L^{-1} Pb; and Zn emission line at 213.856 nm, calibration curve from 0 to 30 Zn mg L^{-1}; all calibration curves gaining R^2 values greater than 0.992). Posteriorly, amount of Pb and Zn desorbed was calculated (Yin et al. 1997) and plotted as cumulative Pb or Zn desorption (in % of the total). The first-order kinetics was used to model the correlation between the amount of PTE desorbed over time, as previously demonstrated (Sparks 2003; Barreto et al. 2023).

The sequential extraction of Pb and Zn was conducted following a modified method from the (Silveira et al. 2006) protocol. Briefly, 1 g of air-dried soil was placed in 50-mL polycarbonate centrifuge tubes and mixed in a stepwise fashion with the following solutions: 0.1 M $CaCl_2$ (15 mL, 2 h at 22 ± 2 °C) to target metals in a exchangeable form (F1); 1 M NaOAC (30 mL, pH 5, 5 h at 22 ± 2 °C) to target carbonate (F2); 40% NaOCl (5 mL, pH 8.5, 30 min at 80 °C) to target organic-matter bound (F3); 0.2 M oxalic acid + 0.2 M NH_4-oxalate (30 mL, pH 3, 2 h at 22 ± 2 °C) to target poor crystalline iron oxide bound (F4); and, finally, the solid fraction was digested by the hydrochloric-nitric acid mix (i.e., EPA3051a (USEPA 2007)) method to measure the residual form (F5). The concentrations of Pb and Zn in each extract were measured by ICP-OES. A post hoc multiple comparison for observed means was carried out in Statistica 13 software (StatSoft Inc.) using Fisher's LSD method at 5% ($p < 0.05$).

Zn spectroscopic speciation

Zn was chosen among the metal contaminants because it was the element with the highest total concentration in the samples, high enough to offer a suitable spectrum quality for XANES analysis. Soil samples that received the highest rate of each amendment were grounded at 50 mesh. The Zn K-edge XANES data was collected at Beamline XAFS2 at the Brazilian Synchrotron Light Laboratory (LNLS, https://lnls.cnpem.br/facilities/xafs2-en/). The Si (111) monochromator energy was calibrated to 9659 eV based on the first inflection point in the K-edge derivative spectra from a Zn foil. Spectra were acquired in fluorescence mode using a Canberra 15-element Ge solid-state detector. We gathered five spectra per sample through the energy range of − 130 to 340 eV in relation to the Zn K-edge energy (E_0 = 9659 eV), with the following energy steps: 0.5 eV in the pre-edge (− 130 to − 35), 0.2 eV across the absorption edge region (− 35 to 65), and 1 eV in the post-edge region (65 to 340) with 1 s of acquisition time.

The scans were merged, aligned, and processed by subtracting the backgrounds using a linear pre-edge function between − 120 and − 45 eV and a linear or quadratic function between + 30 and + 110 eV from E_0, followed by a flattening function in the post-edge region for normalization. Linear combination fitting (LCF) was then performed across the − 20 to + 80 region to identify singular Zn species and their relative proportions on the sample Zn spectrum, following the method described by Manceau et al. (2012). The Zn standards used in this study were previously reported in Khaokaew et al. (2012) (Fig. 5SM). All XANES analysis steps were processed in the Athena Software package (Newville 2001; Ravel and Newville 2005).

Results

Soil and amendment characterization

The amount of Pb present in the soil sample was around 16-fold higher, while the Cd content was around 20-fold higher than the reference quality values suggested by the Environmental Agency of the State of São Paulo (CETESB 2016). These values are considered hazardous as their concentrations exceeded the intervention values accepted for agricultural areas (Table 1). Moreover, the amount of Zn was around 14-fold higher than the reference quality values, surpassing the prevention value, which is a threshold in Brazilian legislation that indicates a high likelihood of damage to suitable soil ecosystem functions and groundwater quality (Table 1) (CETESB 2016). Pb and Zn were not present in the biochar, whereas biosolids had a significant amount of these elements and were slightly alkaline, and both had a high cationic exchange capacity (Table 2).

The phosphate amendments reduced the pH by 0.4 unit, thus concomitantly increasing exchangeable acidity likely because of NH_4^+ oxidation (i.e., from $NH_4H_2PO_4$) (Dong et al. 2021), while lime increased pH by 0.5 unit and biochar by 0.7 pH unit (Table 1). Except for the phosphate addition, the amendments decreased the potential acidity (H + Al) and improved the alkalinity features of the soil. The total carbon contents were significantly increased by biochar (+ 120%) and biosolid treatment (+ 65%), which is expected because the biochar had ~ 65% of C in total elemental composition while biosolids had just 15% (Table 2). The highest phosphate dose increased the P available contents ~ 34 times, and biosolids increased 14 times at the highest rate. Lime

Table 1 Chemical properties[1] of forest soil impacted by atmospheric deposition of mine-waste at distinct dose of phosphate, lime, biosolids, and biochar, after 60 days of incubation

Treatment	pH	C	P	K	Ca	Mg	H + Al	Ex.Ac*	Pb	Cd	Zn
	0.01 M $CaCl_2$	g kg^{-1}	mg kg^{-1}	$mmol_c$ kg^{-1}					mg kg^{-1}		
Control	6.1	43	19	4.6	49	29	18	0.2	270	13.1	858
Phosphate											
Full rate	5.7	40	648	4.6	55	28	29	2.2	270	11.3	820
Half rate	6.0	42	246	4.7	50	27	20	0.7	215	12.2	858
Quarter rate	6.1	41	96	4.1	46	24	20	0.7	223	11.5	823
Lime											
Full rate	6.6	42	26	4.8	82	24	13	0.2	200	11.5	836
Half rate	6.5	36	22	4.7	70	27	15	0.2	220	13.0	915
Quarter rate	6.2	36	20	3.5	58	25	17	0.2	214	10.4	834
Biosolids											
5%	6.5	39	97	8.3	94	59	15	0.2	222	13.8	812
10%	6.6	59	196	13.5	93	58	14	0.1	198	13.5	821
20%	6.8	71	278	19.9	118	67	13	0.1	201	12.1	840
Biochar											
2.5%	6.2	51	29	12.8	50	35	17	0.3	232	11.7	770
5%	6.0	67	37	20.4	46	25	18	0.2	215	12.2	810
10%	5.9	95	45	23.8	48	26	18	0.3	230	13.5	816

*Exchangeable acidity

[1]Standard deviation < 5%, $n = 5$

Table 2 Chemical properties and elemental composition of biochar and biosolids

Amendments	pH[1]	CEC[2]	C[3]	P[4]	K[4]	Ca[4]	Mg[4]	Pb[4]	Cd[4]	Zn[4]
	H_2O	$mmol_c$ kg^{-1}	g kg^{-1}					mg kg^{-1}		
Biosolids	7.4	270	150	7	8	38	13	19.1	< 0.1	314
Biochar	8.8	200	650	2	10	3	3	0.0	0.0	0.03

Standard deviation < 5%, $n = 3$.

[1]pH in a soil/water ratio of 1:2.5

[2]Cation exchange capacity (CEC) by the $BaCl_2$ method.

[3]Shimadzu TOC-5000 carbon analyzer.

[4]EPA3051a method.

and biosolid amendments increased Ca contents by ~ 70% and ~ 144%, respectively (Table 1).

PTE desorption kinetic and sequential extraction

The pseudo-first-order kinetic model reached a good fit to the values of cumulative Zn and Pb (Figs. 1 and 2) extracted by Mehlich-III solution, as shown by the high coefficient of determination (Table 3) and by the low values for reduced χ^2 (Fig. 3SM). The parameters that estimate the constant velocity rate of kinetic (k_1 (min^{-1}), Table 3) were similar in our observations. In general, regardless of the soil amendment, 50% of the total Pb released was released after ~ 28 min, and 50% of the total Zn released was after ~ 19 min. The parameters that estimate the maximum amount of metal release at equilibrium, assuming time $\rightarrow +\infty$, describe the effect of amendment treatments on the metal's solubility.

In the pseudo-first-order kinetic model, $^{*}q_{max}$ means the maximum amount of metal (% of the total metal content presented in Table 1) desorbed at equilibrium, when time (min) $\rightarrow +\infty$; and k_1 (min^{-1}) is the velocity rate constants. $^{**}R^2$ is the coefficient of determination of the model to data fitting. The fitting example is shown in Fig. 3SM. The q_e values followed by the same letter, for each treatment and control, share the same 95% confidence interval. The "aa" letter means that q_e value of this treatment was higher than the q_e value estimated for control.

Lime was the most effective amendment to decrease Zn desorption, reducing it by 17% at full rate, 21% at half rate, and 27% at 1/4 recommended lime dose. Conversely, the addition of phosphate in full rate increased Zn mobility by + 10% (Fig. 1 and Table 3) and was effective in decreasing Pb desorption, reducing it by 17% at full rate, 19% at half rate, and 22% at 1/4 phosphate recommended dose (Fig. 2 and Table 3). On the other hand, lime was not efficient at reducing Pb release at full or half dose. For Pb, the worst amendment was biosolids at a rate of 20%, which increased the Pb released by + 20%. At a 10% biosolid rate, however, the lowest Pb desorption was observed (Fig. 2 and Table 3).

The Zn sequential fractionation stressed only variations in the F1 fraction (Fig. 3), related to the exchangeable, more environmentally available fraction. The values observed in the F1 fraction increased with high phosphate and biochar rates. Lime treatments did not affect Zn fractions, and the addition of biosolids decreased the exchangeable Zn fraction over the rate increment, following the results observed in the desorption experiment (Fig. 1). Otherwise, the proportions of Pb throughout the sequential fractionation were not

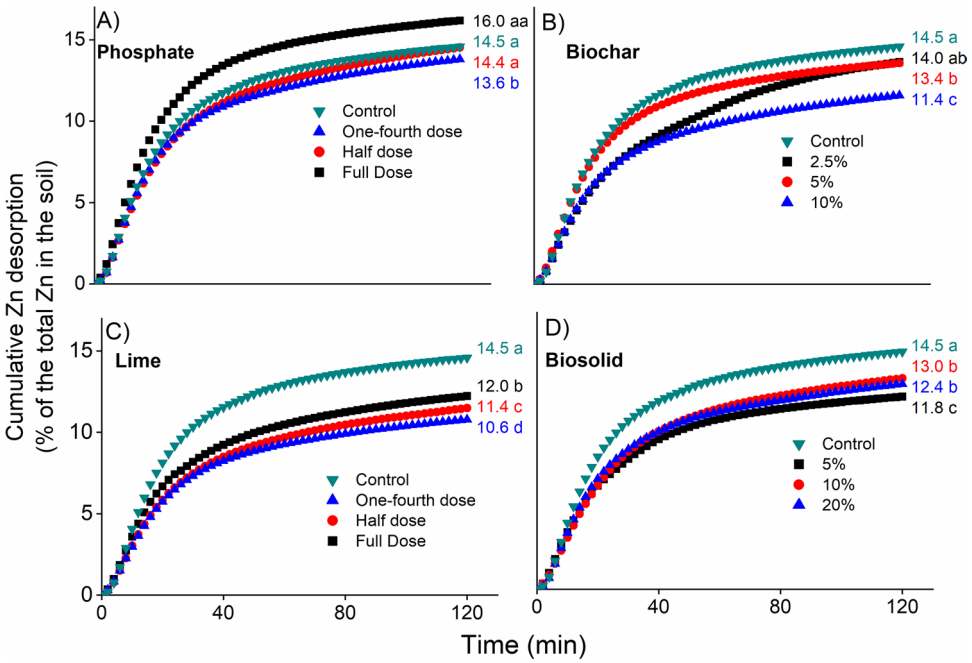

Fig. 1 Experimental data (dots) of cumulative Zn desorption (% of the total Zn in the soil shown in Table 1) by Mehlich-III solution in a stirred flow system. Soil samples were collected in a contaminated forest (control) and after its remediation by **A** phosphate, **B** biochar, **C** lime, and **D** biosolids at different rates. The first-order kinetics was adjusted (see example in Fig. 3SM), and the estimated maximum amount of Zn desorbed (q_{max}) at equilibrium (time $\rightarrow +\infty$) is presented for each treatment. The q_e values followed by the same letter, for each treatment and control, share the same 95% confidence interval. The "aa" later means that q_e value of this treatment was higher than the q_e value estimated for control. The complete results are shown in Table 3

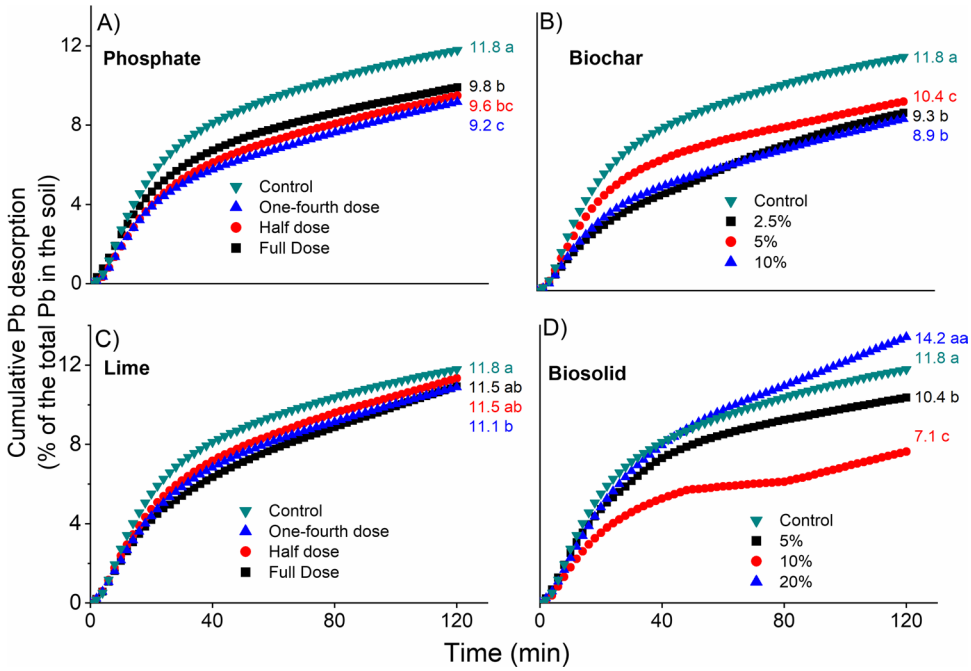

Fig. 2 Experimental data (dots) of cumulative Pb desorption (% of the total Pb in the soil shown in Table 1) by Mehlich-III solution in a stirred flow system. Soil samples were collected in a contaminated forest (control) and after its remediation by **A** phosphate, **B** biochar, **C** lime, and **D** biosolids at different rates. The first-order kinetics was adjusted (see example in Fig. 3SM), and the estimated maximum amount of Pb desorbed (q_{max}) at equilibrium (time $\rightarrow +\infty$) is presented for each treatment. The q_e values followed by the same letter, for each treatment and control, share the same 95% confidence interval. The complete results are shown in Table 3

Table 3 Desorption kinetic parameters of Pb and Zn desorption of the contaminated forest soil (control) and after amendment application

Treatment	Pseudo-first-order kinetic model [$q_t = q_{max} * (1\text{-}\exp^{-k_1 t})$]					
	Pb			Zn		
	q_e* (%)	k_1 (min^{-1})	R^{2**}	q_e (%)	k_1 (min^{-1})	R^2
Control	11.8 **a**	0.029	0.993	14.5 **a**	0.039	0.992
Phosphate						
Full rate	9.8 **b**	0.029	0.993	16.0 **aa**	0.042	0.993
Half rate	9.6 **bc**	0.024	0.993	14.4 **a**	0.034	0.993
Quarter rate	9.2 **c**	0.024	0.989	13.6 **b**	0.038	0.991
Lime						
Full rate	11.5 **ab**	0.020	0.993	12.0 **b**	0.037	0.994
Half rate	11.5 **ab**	0.024	0.994	11.4 **c**	0.034	0.995
Quarter rate	11.1 **b**	0.023	0.994	10.6 **d**	0.036	0.995
Biochar						
2.5%	10.4 **b**	0.015	0.996	14.0 **ab**	0.026	0.996
5%	9.3 **c**	0.029	0.990	13.4 **b**	0.041	0.994
10%	8.9 **c**	0.021	0.990	11.4 **c**	0.036	0.994
Biosolids						
5%	10.4 **b**	0.029	0.997	11.8 **c**	0.037	0.997
10%	7.1 **c**	0.031	0.978	13.0 **b**	0.033	0.996
20%	14.2 **aa**	0.020	0.995	12.4 **b**	0.037	0.993

modified noticeably by soil amendments (Fig. 4SM), and the only exception was the decrease in exchangeable Pb fraction (F1) over the increase in phosphate rate (Fig. 4SM). All these results observed in sequential fractionation agreed with those observed in the desorption experiment (Figs. 1 and 2).

Zn-XAS assessment

The LCF-XANES satisfactorily fitted the sample data, as observed in Fig. 4A, both visually by the low *R* factor value and by the sum value close to 1 (Table 1SM). The primary Zn species in the non-amended soil were Zn-kerolite (2:1 phyllosilicate, 57%), Zn adsorbed at gibbsite (31%),

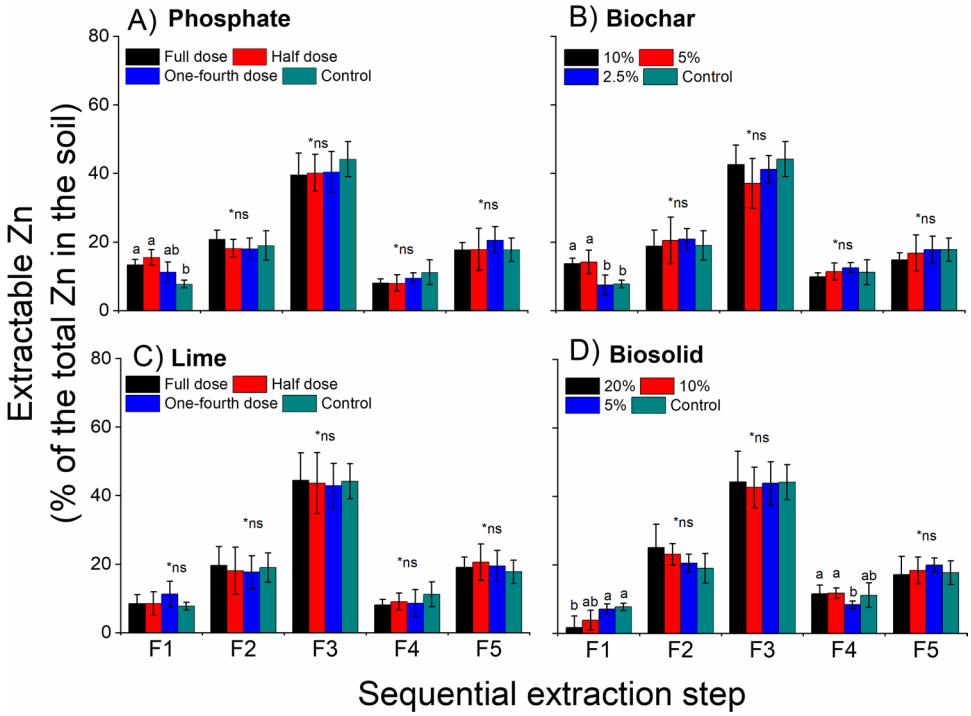

Fig. 3 Relative allocation of Zn among the soil fractions as a function of amendments and rates. F1, exchangeable; F2, carbonate-associated; F3, organic-matter associated; F4, oxide; F5, residual. The relative distribution of Pb is shown in Fig. 4SM. Vertical bars denote stand errors ($n=3$). Bars followed by different letters are different by LSD test ($p<0.05$); otherwise, *ns, not significant

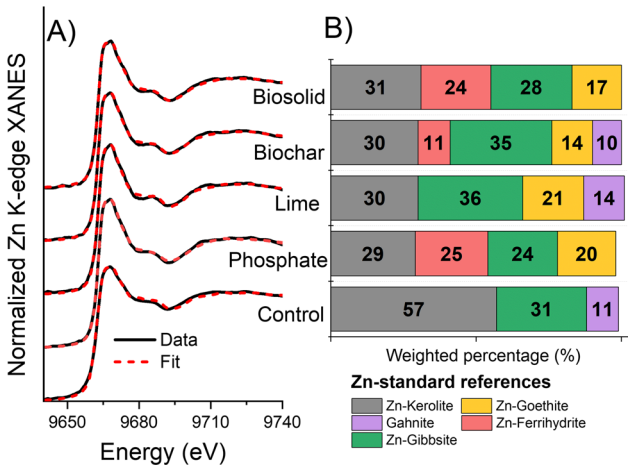

Fig. 4 **A** Normalized Zn K-edge XANES spectra of contaminated forest soil (control) and after 60 days of incubation with the amendments (i.e., phosphate, lime, biochar, and biosolids). The LCF model fits over the energy range from 9639 to 9739 eV (−20 to + 80 eV energy range relative to Zn K-edge ($E_0=9659$ eV)). Black line means the experimental data, and red dotted line presents the LCF model fits. **B** Zn speciation chemical proportion based on Zn-XANES LCF. Details of Zn-standard references in Fig. 4SM. See details about the goodness of fit and uncertainty in Table 1SM

and in a minor part gahnite (ZnAl2O4, 11%) (Fig. 4B and Table 1SM). A strong reduction of Zn-kerolite fraction from 57 to around 30% was observed regardless of the soil amendments, after the incubation. We also observed an occurrence of Zn associated with Fe minerals (goethite and ferrihydrite), reaching 21% after lime treatment, 45% after phosphate, 25% after biochar, and 43% of the Zn-Fe fraction after biosolid reaction in soil. Phosphate and biosolid treatments eliminated the gahnite fraction and reduced the proportion of Zn adsorbed on gibbsite (Fig. 4B and Table 1SM). It was consistent with the decrease in Zn-Al fraction because 42% of Zn-Al was detected in the control treatment (i.e., unamended soil), while this fraction reached 28% after biosolid addition and just 24% after phosphate addition. Conversely, lime increased the Zn-Al fraction to 50%, while biochar maintained it around 45% (Fig. 4B and Table 1SM).

Discussion

The Mehlich-III components react with the soil and quickly enhance ion mobilization by ionic exchange and ion chelation, which may offset in part the restrictions on time-limiting desorption. As Mehlich-III is an efficient extractor for assessing the mobility of PTE in mine residues and contaminated soils, it is employed for measuring their bioavailability (Plunkett et al. 2018) and the efficacy of reclamation strategies for hazardous elements' immobilization (McNear et al. 2007). The desorption kinetics of Zn and Pb in the soil (Figs. 1 and 2 and Table 3) provided valuable insights into their mobility. The desorption of total metal contents was around 15% of the total Zn and 12% Pb. However, the time necessary to release 50% of the total amount of Zn (~ 19 min) is lower than that of Pb (~ 28 min) regardless of the amendments, suggesting that the immobilization features are different between these metals.

The metal adsorption/immobilization in soil has been explained by three molecular mechanisms: (i) nonspecific adsorption when metal is located in the diffuse layer, playing as counter-ions; (ii) specific adsorption on minerals or organic fraction surface complexation (Bowers and Huang 1986; Bradl 2004; Bolan et al. 2014; Uddin 2017); and (iii) at high pH, metal precipitating as hydroxides and (or) as carbonates dominate (Kinniburgh et al. 1976; Yong and Phadungchewit 1993; Bradl 2004). We speculate that Pb is more specifically adsorbed in soil solid surfaces than Zn, which is supported by some researchers that observed a selectivity sequence (i.e., sorption lyotropic series (Kinniburgh et al. 1976)), with Pb being preferentially adsorbed over Zn (Kinniburgh et al. 1976; Elliott et al. 1986; Gomes et al. 2001; Moreira and Alleoni 2010). This difference fate between Zn and Pb is stressed by sequential extraction because, even assuming the same Zn-Pb point source (i.e., mine dust), over time, they migrated to Zn, which had a prevalence with the organic fraction (Fig. 3), while Pb was preferentially associated with the residual fraction (Fig. 4SM). Thus, a possible Zn-Pb interaction on soil immobilization or leaching was lacking in experimental evidence. Future studies in μ-scale analysis (e.g., μ-XRF/XAS/XRD) should consider this possibility.

The addition of lime effectively decreased Zn availability (Fig. 1 and Table 3). We suggest that the increment in the pH values to 6.5–6.6 (Table 1) likely deprotonated the soil-solid surfaces and, consequently, improved the effective CEC (Table 1), thus improving the electrostatic affinity between soil particles and Zn ions. It is possible that the amount of Ca added to the system was not sufficient to compete with Zn for adsorption sites (Escrig and Morell 1998). On the other hand, Pb desorption was not affected in the same extension by lime treatment because its specific adsorption mechanism is less pH-dependent than Zn (Harter 1983; Bradl 2004), likely because Pb presents a higher electronegativity (Pb^{2+} = 1.87 arbitrary units) than Zn (Zn^{2+} = 1.65 arbitrary units) (Pan et al. 2022).

Phosphate amendment was able to decrease Pb desorption (Fig. 2), confirming our previous study, which demonstrated that phosphate and lime amendments decreased Pb mobility due to the formation of pyromorphite-like (i.e., $Pb_5(PO_4)_3Cl$), a stable and insoluble mineral, as observed on Pb-XANES data (Gomes et al. 2022). An additional possibility is the establishment of ternary complex among "mineral surface–phosphate–metal" was formed, which could strengthen the stability of ion adsorption complexes through chemical bonds between metal and ligand surface (Elzinga and Kretzschmar 2013; Ren et al. 2015; Liu et al. 2016). On the other hand, the full dose of phosphate amendment increased Zn desorption (Fig. 1). This is likely due to the presence of ammonium ($NH_4H_2PO_4$) in the P source, which after NH_4^+ oxidation to nitrate causes a decrease in pH values (Bouman et al. 1995; Hu et al. 2014). This increase in soil acidity increased the H + activity in the soil solution, consequently displacing Zn ions from the surface of soil colloids and increasing their mobility (Fig. 1).

Biochar and biosolids have high CECs and alkalinity properties (Table 2), which explain the Zn immobilization in their applications. Phosphate, biochar, and 5 and 10% of biosolids promoted a consistent decrease in Pb desorption (Fig. 2 and Table 3). We suggest that the forest soil studied here had a strong buffer capacity, likely due to the higher clay content (77%) than mine-waste impacted soil (13%, Gomes et al. (2022)), which is a crucial parameter for immobilizing soluble organics released by biochar and biosolids (Jardine et al. 1989; Kalbitz et al. 2000; Barreto et al. 2021). However, at a 20% rate, the addition of biosolids increased Pb desorption, probable surpassing the soil's buffer capacity, increasing the metal mobility by soluble organo-Pb complexes. Evidence of the higher buffer capacity of the forest soil is supported by the results of sequential extraction fractionation (Fig. 3 and Fig. 4SM). For Zn, only the F1 fraction changed as a result of the amendments and rates applied, while the treatments kept similar features of the original control soil (Fig. 3). For Pb, the F2 fraction after phosphate addition showed a significant difference when compared to the control soil. Beyond clay content, the high content of soil organic matter present in the original soil also had a strong bearing effect on Zn (Fan et al. 2016) and Pb (Strawn and Sparks 2000). Silicate minerals and soil organic matter could prevent strong variations in the metal distribution, as observed over sequential extractions.

The LCF of XANES data suggests Zn-kerolite as the major species in the non-amended soil (57%), and ca. 30% after the treatments at the higher rates (Fig. 4). Zn-kerolite had been identified in previous studies (Voegelin et al. 2008, 2011; Jacquat et al. 2009) as a proxy for Zn-phyllosilicates. We suppose that this Zn-silicate fraction is part of the original mine dust that originally contaminated the area because the Vazante mine primarily contained Zn-silicates such as willemite (Zn_2SiO_4) in the ore (Monteiro et al. 1999; Babinski et al. 2005). Nachtegaal and Sparks (2004) observed the Zn complex developing at the goethite-coated kaolinite surface at pH 7.0, which is a system comparable to our real soil system, and after aging for 45 days, they concluded that precipitation at the kaolinite surface was thermodynamically preferred over adsorption to the goethite coating. Over the years of aging, any Zn released by mine dust would have been re-precipitated as Zn-rich phyllosilicate, such as Zn-kerolite species (Panfili et al. 2005; Nachtegaal et al. 2005). It is noteworthy that the stability of Zn-kerolite and other Zn-bearing phases was discussed by Jacquat et al. (2008), who observed that synthetic Zn-kerolite added to pristine soil was removed by 1 M NH_4NO_3 followed by 1 M NH_4-acetate at pH 6.0, which is in agreement

with the sequential extraction procedure (Fig. 3). Therefore, the changes in soil chemical equilibrium after soil amendment application likely led to a Zn-kerolite replacement for Zn-Fe species, especially after phosphate and biosolid amendments.

Due to the increased availability of phosphate and biosolids, we suggested that the Zn-Fe feature is a result of ternary complex formation, as previously observed in soil (Bolland et al. 1977; Agbenin 1998) and also in the purified system for ferrihydrite (Liu et al. 2016; Van Eynde et al. 2022). The correlation of this observation with desorption data of soil samples amended with phosphate (i.e., the highest rate) suggests that this new Zn-Fe phase is prone to solubilization; however, the data of biosolids does not totally support this assumption. On the other hand, biochar and lime preserved a high proportion of Zn-Al species, which are not associated with high (or easy) Zn desorption. The alkalinity produced by lime decomposition and biochar immobilization of H^+ from the media (Xiao and Pignatello 2015; Ahmed et al. 2018; Zhang et al. 2018) likely contributed to the stability of Zn-Al species.

The high C content in the forest soil presented in this study (4 g kg^{-1} of total C, Table 1), might offer a stable and insoluble PTE-organic complex (Ahmad et al. 2016; Li et al. 2022). This stabilization is less prone in our previous study (1.5 g kg^{-1} of total C). Thus, soil management that decreases soil C content might increase PTE mobility. Beyond C, the heavily contaminated soil/sediment in the mine site presented a lower buffer capacity for Pb remobilization after biochar and biosolid addition, likely because of the lower proportion of Fe and Al oxyhydroxides that are strong sinks of soluble organic-mineral complexes. Thus, we outlined that the physiochemical properties such as mineralogy composition and soil C content, beyond the level PTE contamination, should be observed to predict the efficiency of remediation practices.

Environmental implications and conclusions

The use of soil amendments has been shown to enhance the adsorption of PTE, thus decreasing its easily mobile fraction. The selection of the most suitable soil amendment is initially predicted and/or tested in simplified systems, for example, observing the behavior of single contaminant in purified materials, such as clays and, or Fe/Al oxyhydroxides. However, the situation is more complex at real contaminated sites, where several possibilities of chemical reactions might happen, and often, there is more than one PTE that needs to be immobilized. In the case of the forest soil evaluated here, the results of PTE desorption by stirred flow indicate that only around 11% of the total Pb or Zn amount could be removed after long-term desorption. Consequently, 89% was immobile, which could be seen as a metal soil compartment of low risk for environmental implications.

Our observations suggest that phosphate addition kept Pb less available, in agreement with our previous study; however, it increased Zn desorption. Thus, it is necessary to be aware of the possible incompatibility of soil recommendations based on heavily contaminated mine sediments (i.e., contaminations in a few gram per kilogram) and recommendations destined for contaminated soil (i.e., contaminations in milligram per kilogram). Based on our studies, the addition of lime seems to be a suitable option as it decreases Zn and Pb releases. However, the life span of the lime reaction is limited by the acidification of the soil (Guo et al. 2010). It hinders a good prediction of soil remediation success over the long term. Aligning our studies, the most suitable strategy might be combining the soil amendments, for instance, initially applying phosphate to immobilize Pb by pyromorphite precipitation (Gomes et al. 2022), and then applying lime focused to reduce Zn solubility (Fig. 1). This alternative should be considered in future studies.

We conclude that lime is a suitable option for most soil remediation cases. We endorse the necessity to observe these amendments, or a combination of them, in long-term field trials to avoid overestimating laboratory results and to confirm the amendment efficiency against PTE remobilization by weather (e.g., precipitation) and vegetation life cycle (i.e., root exudation, litter decay, and biomass decomposition). Thus, it leads to a better decision on multiple PTE remediation for long-term scenarios.

Supplementary Information The online version contains supplementary material available at https://doi.org/10.1007/s11356-023-30643-0.

Acknowledgements We are also thankful to Professor Leônidas Carrijo Azevedo Melo and Professor Luiz Roberto Guimarães Guilherme (Soil Science Department at Federal University of Lavras (UFLA, Brazil)), for kindly providing the soil samples, and Professor Leonardus Vergutz (Mohammed VI Polytechnique University, Morocco), for his support in the stirred flow investigation. We are also grateful to Professor Donald Sparks group's (Environmental Soil Chemistry Lab, University of Delaware, USA) for providing the data of Zn-XANES standards. The XAFS2 beamline staff is acknowledged for their support throughout the experiments. The authors also thank Professor Dean Hesterberg (North Caroline State University/Brazilian Synchrotron Light Laboratory) for his valorous comments throughout this manuscript and thank the valorous comments offered by anonymous reviewers.

Author contribution Conceptualization: M. S. C. B. and F. P.G.; methodology: M. S. C. B. and F. P. G.; formal analysis: M. S. C. B., F. P. G., and H. W. P. C.; investigation: M. S. C. B., F. P. G., and H. W. P. C.; writing—original draft: all authors; writing—review and editing: M. S. C. B.; supervision: H. W. P. C. and L. R. F. A.; project administration and funding acquisition: H. W. P. C. and L. R. F. A

Funding We gratefully acknowledge the generous scholarships provided by the São Paulo Research Foundation (FAPESP) to MSCB (grants #2016/05870–1 and #2016/22058–9) and FPG (grants #2016/13734–0 and #2017/11700–4). HWPC (grant #306185/2020–2) and LRFA (grant #306429/2018–7) thanks CNPq (Conselho Nacional

de Desenvolvimento Científico e Tecnológico), Brazil, for research productivity fellowships. Furthermore, we are grateful to CAPES (Coordenação de Aperfeiçoamento de Pessoal de Nível Superior), Brazil (Finance Code 001), for their financial support. This research was made possible by the resources of the Brazilian Synchrotron Light Laboratory (LNLS) (proposal number: #20170360), an open national facility managed by the Brazilian Centre for Research in Energy and Materials (CNPEM), of the Brazilian Ministry for Science, Technology and Innovations (MCTI).

Data Availability The datasets used in this manuscript are available upon request.

Declarations

Ethics approval This section is not applicable in this document.

Consent to participate All authors involved in this paper have confirmed their participation in the experimental study and the preparation of the paper.

Consent for publication All authors approved the paper for publication.

Conflict of interest The authors declare no competing interests.

References

Agbenin JO (1998) Phosphate-induced zinc retention in a tropical semi-arid soil. Eur J Soil Sci 49:693–700. https://doi.org/10.1046/j.1365-2389.1998.4940693.x

Ahmad M, Ok YS, Rajapaksha AU et al (2016) Lead and copper immobilization in a shooting range soil using soybean stover- and pine needle-derived biochars: chemical, microbial and spectroscopic assessments. J Hazard Mater 301:179–186. https://doi.org/10.1016/j.jhazmat.2015.08.029

Ahmed MB, Zhou JL, Ngo HH et al (2018) Sorption of hydrophobic organic contaminants on functionalized biochar: protagonist role of π-π electron-donor-acceptor interactions and hydrogen bonds. J Hazard Mater 360:270–278. https://doi.org/10.1016/j.jhazmat.2018.08.005

Ali A, Shaheen SM, Guo D et al (2020) Apricot shell- and apple tree-derived biochar affect the fractionation and bioavailability of Zn and Cd as well as the microbial activity in smelter contaminated soil. Environ Pollut 264:114773. https://doi.org/10.1016/j.envpol.2020.114773

Ali SH, Giurco D, Arndt N et al (2017) Mineral supply for sustainable development requires resource governance. Nature 543:367–372. https://doi.org/10.1038/nature21359

Babinski M, Monteiro LVS, Fetter AH et al (2005) Isotope geochemistry of the mafic dikes from the Vazante nonsulfide zinc deposit, Brazil. J South Am Earth Sci 18:293–304. https://doi.org/10.1016/j.jsames.2004.11.010

Barreto MSC, Elzinga EJ, Ramlogan M et al (2021) Calcium enhances adsorption and thermal stability of organic compounds on soil minerals. Chem Geol 559:119804. https://doi.org/10.1016/j.chemgeo.2020.119804

Barreto MSC, Elzinga EJ, Sparks DL (2023) The adsorption of arsenate and p-arsanilic acid onto ferrihydrite and subsequent desorption by sulfate and artificial seawater: future implications of sea level rise. Environ Pollut 121302. https://doi.org/10.1016/j.envpol.2023.121302

Basta NT, Gradwohl R, Snethen KL, Schroder JL (1997) Chemical immobilization of lead, zinc, and cadmium in smelter-contaminated soils using biosolids and rock phosphate. J Environ Qual 30:1222–1230. https://doi.org/10.2134/jeq2001.3041222x

Basta NT, McGowen SL (2004) Evaluation of chemical immobilization treatments for reducing heavy metal transport in a smelter-contaminated soil. Environ Pollut 127:73–82. https://doi.org/10.1016/S0269-7491(03)00250-1

Bolan N, Kunhikrishnan A, Thangarajan R et al (2014) Remediation of heavy metal (loid) s contaminated soils – to mobilize or to immobilize ? J Hazard Mater 266:141–166. https://doi.org/10.1016/j.jhazmat.2013.12.018

Bolan NS, Adriano DC, Naidu R (2003) Role of phosphorus in (Im) mobilization and bioavailability of heavy metals in the soil-plant system. Rev Environ Contam Toxicol 177:1–44

Bolland M, Posner A, Quirk J (1977) Zinc adsorption by goethite in the absence and presence of phosphate. Soil Res 15:279. https://doi.org/10.1071/SR9770279

Bouman OT, Curtin D, Campbell CA et al (1995) Soil acidification from long-term use of anhydrous ammonia and urea. Soil Sci Soc Am J 59:1488–1494. https://doi.org/10.2136/sssaj1995.03615995005900050039x

Bowers A, Huang C (1986) Adsorption characteristics of metal-EDTA complexes onto hydrous oxides. J Colloid Interface Sci 110:575–590. https://doi.org/10.1016/0021-9797(86)90410-8

Bradl HB (2004) Adsorption of heavy metal ions on soils and soils constituents. J Colloid Interface Sci 277:1–18. https://doi.org/10.1016/j.jcis.2004.04.005

Brazilian Economy Ministry (2022) Foreign trade statistics—history series.

Cao X, Wahbi A, Ma L et al (2009) Immobilization of Zn, Cu, and Pb in contaminated soils using phosphate rock and phosphoric acid. J Hazard Mater 164:555–564. https://doi.org/10.1016/j.jhazmat.2008.08.034

CETESB CA do E de SP (2016) Decisão de Diretoria nº 256/2016/E - Dispõe sobre a aprovação dos "Valores Orientadores para Solos e Águas Subterrâneas no Estado de São Paulo - 2016". See at https://cetesb.sp.gov.br/aguas-subterraneas/wp-content/uploads/sites/13/2013/11/dd256_2016_e_valoresorientadoresdioxinasefuranos2016.pdf (in Portuguese)

Chen L, Zhou M, Wang J et al (2022) A global meta-analysis of heavy metal(loid)s pollution in soils near copper mines: evaluation of pollution level and probabilistic health risks. Sci Total Environ 835:155441. https://doi.org/10.1016/j.scitotenv.2022.155441

Dong Y, Yang J-L, Zhao X-R et al (2021) Contribution of different proton sources to the acidification of red soil with maize cropping in subtropical China. Geoderma 392:114995. https://doi.org/10.1016/j.geoderma.2021.114995

Elkhatib EA, Moharem ML (2015) Immobilization of copper, lead, and nickel in two arid soils amended with biosolids: effect of drinking water treatment residuals. J Soils Sediments 15:1937–1946. https://doi.org/10.1007/s11368-015-1127-1

Elliott HA, Liberati MR, Huang CP (1986) Competitive adsorption of heavy metals by soils. J Environ Qual 15:214–219. https://doi.org/10.2134/jeq1986.00472425001500030002x

Elzinga EJ, Kretzschmar R (2013) In situ ATR-FTIR spectroscopic analysis of the co-adsorption of orthophosphate and Cd(II) onto hematite. Geochim Cosmochim Acta 117:53–64. https://doi.org/10.1016/j.gca.2013.04.003

Entwistle JA, Hursthouse AS, Marinho Reis PA, Stewart AG (2019) Metalliferous mine dust: human health impacts and the potential determinants of disease in mining communities. Curr Pollut Reports 5:67–83. https://doi.org/10.1007/s40726-019-00108-5

Escrig I, Morell I (1998) Effect of calcium on the soil adsorption of cadmium and zinc in some Spanish sandy soils. Water Air Soil Pollut 105:507–520. https://doi.org/10.1023/A:1004919807528

Ettler V (2016) Soil contamination near non-ferrous metal smelters: a review. Appl Geochemistry 64:56–74. https://doi.org/10.1016/j.apgeochem.2015.09.020

Fan T-T, Wang Y-J, Li C-B et al (2016) Effect of organic matter on sorption of Zn on soil: elucidation by Wien effect measurements and EXAFS spectroscopy. Environ Sci Technol 50:2931–2937. https://doi.org/10.1021/acs.est.5b05281

Fang S, Tsang DCW, Zhou F et al (2016) Stabilization of cationic and anionic metal species in contaminated soils using sludge-derived biochar. Chemosphere 149:263–271. https://doi.org/10.1016/j.chemosphere.2016.01.060

Federal Remediation Technologies Roundtable (2009) Remediation technologies screening matrix and reference guide - version 4.0. In: Remediat. Technol. Screen. Matrix Ref. Guid. See at https://frtr.gov/matrix2/top_page.html

Feola Conz R, Abbruzzini TF, de Andrade CA et al (2017) Effect of pyrolysis temperature and feedstock type on agricultural properties and stability of biochars. Agric Sci 08:914–933. https://doi.org/10.4236/as.2017.89067

Gao J, Han H, Gao C et al (2023) Organic amendments for in situ immobilization of heavy metals in soil: a review. Chemosphere 335:139088. https://doi.org/10.1016/j.chemosphere.2023.139088

Gardioli LFN, Fialho RC, Barreto MSC et al (2023) N fertilization did not raise soil greenhouse gas emissions in a reforested reclaimed-mine site over a short-term study. Ecol Eng 194:107040. https://doi.org/10.1016/j.ecoleng.2023.107040

Gomes FP, Barreto MSC, Amoozegar A, Alleoni LRF (2022) Immobilization of lead by amendments in a mine-waste impacted soil: assessing Pb retention with desorption kinetic, sequential extraction and XANES spectroscopy. Sci Total Environ 807:150711. https://doi.org/10.1016/j.scitotenv.2021.150711

Gomes PC, Fontes MPF, da Silva AG et al (2001) Selectivity sequence and competitive adsorption of heavy metals by Brazilian soils. Soil Sci Soc Am J 65:1115–1121. https://doi.org/10.2136/sssaj2001.6541115x

Guo JH, Liu XJ, Zhang Y et al (2010) Significant acidification in major Chinese croplands. Science 327:1008–1010. https://doi.org/10.1126/science.1182570

Harter RD (1983) Effect of soil pH on adsorption of lead, copper, zinc, and nickel. Soil Sci Soc Am J 47:47–51. https://doi.org/10.2136/sssaj1983.03615995004700010009x

He M, Shi H, Zhao X et al (2013) Immobilization of Pb and Cd in contaminated soil using nano-crystallite hydroxyapatite. Procedia Environ Sci 18:657–665. https://doi.org/10.1016/j.proenv.2013.04.090

Hu H-W, Xu Z-H, He J-Z (2014) Ammonia-oxidizing archaea play a predominant role in acid soil nitrification, pp 261–302. https://doi.org/10.1016/B978-0-12-800137-0.00006-6

Jacquat O, Voegelin A, Kretzschmar R (2009) Local coordination of Zn in hydroxy-interlayered minerals and implications for Zn retention in soils. Geochim Cosmochim Acta 73:348–363. https://doi.org/10.1016/J.GCA.2008.10.026

Jacquat O, Voegelin A, Villard A et al (2008) Formation of Zn-rich phyllosilicate, Zn-layered double hydroxide and hydrozincite in contaminated calcareous soils. Geochim Cosmochim Acta 72:5037–5054. https://doi.org/10.1016/J.GCA.2008.07.024

Jardine PM, McCarthy JF, Weber NL (1989) Mechanisms of dissolved organic carbon adsorption on soil. Soil Sci Soc Am J 53:1378–1385. https://doi.org/10.2136/sssaj1989.03615995005300050013x

Kalbitz K, Solinger S, Park JH et al (2000) Controls on the dynamics dissolved organic matter in soils: a review. Soil Sci. https://doi.org/10.1097/00010694-200004000-00001

Kalisz S, Kibort K, Mioduska J et al (2022) Waste management in the mining industry of metals ores, coal, oil and natural gas - a review. J Environ Manage 304:114239. https://doi.org/10.1016/j.jenvman.2021.114239

Kennedy J, Dean J, Okeme I, Sapsford D (2023) An assessment of the efficacy of sodium carbonate for semi-passive treatment of circumneutral zinc-bearing mine waters. J Water Process Eng 53:103764. https://doi.org/10.1016/j.jwpe.2023.103764

Khaokaew S, Landrot G, Chaney RL et al (2012) Speciation and release kinetics of zinc in contaminated paddy soils. Environ Sci Technol 46:3957–3963. https://doi.org/10.1021/es204007t

Kinniburgh DG, Jackson ML, Syers JK (1976) Adsorption of alkaline earth, transition, and heavy metal cations by hydrous oxide gels of iron and aluminum. Soil Sci Soc Am J 40:796–799. https://doi.org/10.2136/sssaj1976.03615995004000050047x

Kumpiene J, Lagerkvist A, Maurice C (2008) Stabilization of As, Cr, Cu, Pb and Zn in soil using amendments - a review. Waste Manag 28:215–225. https://doi.org/10.1016/j.wasman.2006.12.012

Lee SH, Lee JS, Jeong Choi Y, Kim JG (2009) In situ stabilization of cadmium-, lead-, and zinc-contaminated soil using various amendments. Chemosphere 77:1069–1075. https://doi.org/10.1016/j.chemosphere.2009.08.056

Li Q, Wang Y, Li Y et al (2022) Speciation of heavy metals in soils and their immobilization at micro-scale interfaces among diverse soil components. Sci Total Environ 825:153862. https://doi.org/10.1016/j.scitotenv.2022.153862

Li Y, Ye Z, Yu Y et al (2023) A combined method for human health risk area identification of heavy metals in urban environments. J Hazard Mater 449:131067. https://doi.org/10.1016/j.jhazmat.2023.131067

Liao X, Li Y, Miranda-Avilés R et al (2022) In situ remediation and ex situ treatment practices of arsenic-contaminated soil: an overview on recent advances. J Hazard Mater Adv 8:100157. https://doi.org/10.1016/j.hazadv.2022.100157

Liu J, Zhu R, Xu T et al (2016) Co-adsorption of phosphate and zinc(II) on the surface of ferrihydrite. Chemosphere 144:1148–1155. https://doi.org/10.1016/j.chemosphere.2015.09.083

Madejón E, Doronila AI, Sanchez-Palacios JT et al (2010) Arbuscular mycorrhizal fungi (AMF) and biosolids enhance the growth of a native Australian grass on sulphidic gold mine tailings. Restor Ecol 18:175–183. https://doi.org/10.1111/j.1526-100X.2009.00610.x

Manceau A, Marcus MA, Grangeon S (2012) Determination of Mn valence states in mixed-valent manganates by XANES spectroscopy. Am Mineral 97:816–827. https://doi.org/10.2138/am.2012.3903

MAPA (2014) Manual de métodos analíticos oficiais para fertilizante e corretivos manual de métodos analíticos oficiais para fertilizantes e corretivos. See at https://www.gov.br/agricultura/pt-br/assuntos/insumos-agropecuarios/insumos-agricolas/fertilizantes/legislacao/manual-de-metodos_2017_isbn-978-85-7991-109-5.pdf

Martin TA, Ruby MV (2004) Review of in situ remediation technologies for lead, zinc, and cadmium in soil. Remediation 14:35–53. https://doi.org/10.1002/rem.20011

McNear DH, Chaney RL, Sparks DL (2007) The effects of soil type and chemical treatment on nickel speciation in refinery enriched soils: a multi-technique investigation. Geochim Cosmochim Acta 71:2190–2208. https://doi.org/10.1016/j.gca.2007.02.006

Monteiro LVS, Bettencourt JS, Spiro B et al (1999) The Vazante zinc mine, Minas Gerais, Brazil: constraints on willemitic mineralization and fluid evolution. Explor Min Geol 8:21–42

Moreira CS, Alleoni LRF (2010) Adsorption of Cd, Cu, Ni and Zn in tropical soils under competitive and non-competitive systems. Sci Agric 67:301–307. https://doi.org/10.1590/S0103-90162010000300008

Nachtegaal M, Marcus MA, Sonke JE et al (2005) Effects of in situ remediation on the speciation and bioavailability of zinc in a smelter contaminated soil. Geochim Cosmochim Acta 69:4649–4664. https://doi.org/10.1016/J.GCA.2005.05.019

Nachtegaal M, Sparks DL (2004) Effect of iron oxide coatings on zinc sorption mechanisms at the clay-mineral/water interface. J Colloid Interface Sci 276:13–23. https://doi.org/10.1016/j.jcis.2004.03.031

Naz A, Chowdhury A, Mishra BK, Karthikeyan K (2018) Distribution of heavy metals and associated human health risk in mine, agricultural and roadside soils at the largest chromite mine of India. Environ Geochem Health 40:2155–2175. https://doi.org/10.1007/s10653-018-0090-3

Newville M (2001) IFEFFIT: Interactive XAFS analysis and FEFF fitting. J Synchrotron Radiat 8:322–324. https://doi.org/10.1107/S0909049500016964

Ono FB, Tappero R, Sparks D, Guilherme LRG (2016) Investigation of arsenic species in tailings and windblown dust from a gold mining area. Environ Sci Pollut Res 23:638–647. https://doi.org/10.1007/s11356-015-5304-y

Pan J, Gao B, Guo K et al (2022) Insights into selective adsorption mechanism of copper and zinc ions onto biogas residue-based adsorbent: theoretical calculation and electronegativity difference. Sci Total Environ 805:150413. https://doi.org/10.1016/j.scitotenv.2021.150413

Panfili F, Manceau A, Sarret G et al (2005) The effect of phytostabilization on Zn speciation in a dredged contaminated sediment using scanning electron microscopy, X-ray fluorescence, EXAFS spectroscopy, and principal components analysis. Geochim Cosmochim Acta 69:2265–2284. https://doi.org/10.1016/j.gca.2004.10.017

Pansu M, Gautheyrou J (2007) Handbook of soil analysis. mineralogical, organic and inorganic methods. By M. Pansu and J. Gautheyrou. Berlin, Heidelberg, New York: Springer (2006), pp. 993, £191.50. ISBN 978–3–540–31210–9. Exp Agric 43:401. https://doi.org/10.1017/S0014479707005042

Plunkett SA, Wijayawardena MAA, Naidu R et al (2018) Use of routine soil tests to estimate Pb bioaccessibility. Environ Sci Technol 52:12556–12562. https://doi.org/10.1021/acs.est.8b02633

Puga AP, Abreu CA, Melo LCA et al (2015) Cadmium, lead, and zinc mobility and plant uptake in a mine soil amended with sugarcane straw biochar. Environ Sci Pollut Res 22:17606–17614. https://doi.org/10.1007/s11356-015-4977-6

Puga AP, Melo LCA, de Abreu CA, Coscione AR (2016) Leaching and fractionation of heavy metals in mining soils amended with biochar. Soil Tillage Res 164:25–33. https://doi.org/10.1016/j.still.2016.01.008

Rajendran S, Priya TAK, Khoo KS et al (2022) A critical review on various remediation approaches for heavy metal contaminants removal from contaminated soils. Chemosphere 287:132369. https://doi.org/10.1016/j.chemosphere.2021.132369

Ravel B, Newville M (2005) ATHENA, ARTEMIS, HEPHAESTUS : data analysis for X-ray absorption spectroscopy using IFEFFIT. J Synchrotron Radiat 12:537–541. https://doi.org/10.1107/S0909049505012719

Reddy KR, Cameselle C (2009) Electrochemical remediation technologies for polluted soils, sediments and groundwater. https://doi.org/10.1002/9780470523650

Ren X, Tan X, Hayat T et al (2015) Co-sequestration of Zn(II) and phosphate by γ-Al2O3: from macroscopic to microscopic investigation. J Hazard Mater 297:134–145. https://doi.org/10.1016/j.jhazmat.2015.04.079

Robinson BH, Anderson CWN, Dickinson NM (2015) Phytoextraction: where's the action? J Geochemical Explor 151:34–40. https://doi.org/10.1016/j.gexplo.2015.01.001

Silveira ML, Alleoni LRF, O'Connor GA, Chang AC (2006) Heavy metal sequential extraction methods-a modification for tropical soils. Chemosphere 64:1929–1938. https://doi.org/10.1016/j.chemosphere.2006.01.018

Sparks DL (2003) Enviromental soil chemistry. Elsevier

Strawn DG, Sparks DL (2000) Effects of soil organic matter on the kinetics and mechanisms of Pb(II) sorption and desorption in soil. Soil Sci Soc Am J 64:144–156. https://doi.org/10.2136/sssaj2000.641144x

Uddin MK (2017) A review on the adsorption of heavy metals by clay minerals, with special focus on the past decade. Chem Eng J 308:438–462. https://doi.org/10.1016/j.cej.2016.09.029

USEPA (2004) Risk assessment guidance for superfund (RAGS). Volume I. Human health evaluation manual (HHEM). Part E. Supplemental guidance for dermal risk assessment. Us Epa 1.: EPA/540/1–89/002. See at https://www.epa.gov/sites/default/files/2015-09/documents/rags_a.pdf

USEPA (2007) Microwave assisted acid digestion of sediments, sludges, soils, and oils. Washington, DC. See at https://www.epa.gov/sites/default/files/2015-12/documents/3051a.pdf

Van Eynde E, Hiemstra T, Comans RNJ (2022) Interaction of Zn with ferrihydrite and its cooperative binding in the presence of PO_4. Geochim Cosmochim Acta 320:223–237. https://doi.org/10.1016/j.gca.2022.01.010

Vareda JP, Valente AJM, Durães L (2019) Assessment of heavy metal pollution from anthropogenic activities and remediation strategies: a review. J Environ Manage 246:101–118. https://doi.org/10.1016/j.jenvman.2019.05.126

Voegelin A, Jacquat O, Pfister S et al (2011) Time-dependent changes of zinc speciation in four soils contaminated with zincite or sphalerite. Environ Sci Technol 45:255–261. https://doi.org/10.1021/es101189d

Voegelin A, Tokpa G, Jacquat O et al (2008) Zinc fractionation in contaminated soils by sequential and single extractions: influence of soil properties and zinc content. J Environ Qual 37:1190. https://doi.org/10.2134/jeq2007.0326

Vrînceanu NO, Motelică DM, Dumitru M et al (2019) Assessment of using bentonite, dolomite, natural zeolite and manure for the immobilization of heavy metals in a contaminated soil: the Copșa Mică case study (Romania). CATENA 176:336–342. https://doi.org/10.1016/j.catena.2019.01.015

Wan X, Lei M, Chen T (2016) Cost–benefit calculation of phytoremediation technology for heavy-metal-contaminated soil. Sci Total Environ 563–564:796–802. https://doi.org/10.1016/j.scitotenv.2015.12.080

Wang L, Cho D-W, Tsang DCW et al (2019) Green remediation of As and Pb contaminated soil using cement-free clay-based stabilization/solidification. Environ Int 126:336–345. https://doi.org/10.1016/j.envint.2019.02.057

Xiao F, Pignatello JJ (2015) $\pi + -\pi$ interactions between (hetero) aromatic amine cations and the graphitic surfaces of pyrogenic carbonaceous materials. Environ Sci Technol 49:906–914. https://doi.org/10.1021/es5043029

Yin Y, Allen HE, Huang CP et al (1997) Kinetics of mercury(II) adsorption and desorption on soil. Environ Sci Technol 31:496–503. https://doi.org/10.1021/es9603214

Yong RN, Phadungchewit Y (1993) pH influence on selectivity and retention of heavy metals in some clay soils. Can Geotech J 30:821–833. https://doi.org/10.1139/t93-073

Zhai X, Li Z, Huang B et al (2018) Remediation of multiple heavy metal-contaminated soil through the combination of soil washing and in situ immobilization. Sci Total Environ 635:92–99. https://doi.org/10.1016/j.scitotenv.2018.04.119

Zhang Y, Xu X, Cao L et al (2018) Characterization and quantification of electron donating capacity and its structure dependence in biochar derived from three waste biomasses. Chemosphere 211:1073–1081. https://doi.org/10.1016/j.chemosphere.2018.08.033